

ENVIRONMENTAL INFLUENCES ON ARCTIC HALOGEN CHEMISTRY:
INVESTIGATION OF MELT ONSET AND SNOWPACK PROPERTIES


By

Justine Amanda Burd


RECOMMENDED:



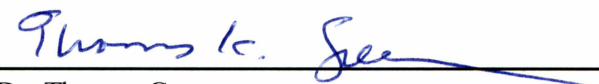
Dr. Thomas Douglas



Dr. Thomas Trainor




Dr. William Simpson
Advisory Committee Chair

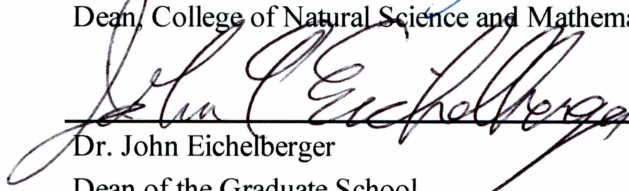


Dr. Thomas Green
Chair, Department of Chemistry and Biochemistry

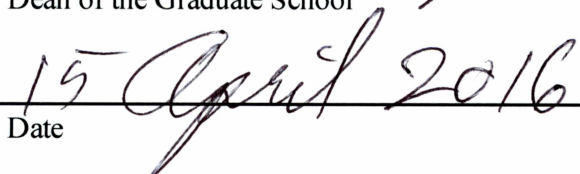
APPROVED:



Dr. Paul Layer
Dean, College of Natural Science and Mathematics



Dr. John Eichelberger
Dean of the Graduate School



Date

ENVIRONMENTAL INFLUENCES ON ARCTIC HALOGEN CHEMISTRY:
INVESTIGATION OF MELT ONSET AND SNOWPACK PROPERTIES

A
THESIS

Presented to the Faculty
of the University of Alaska Fairbanks

in Partial Fulfillment of the Requirements
for the Degree of

MASTER OF SCIENCE

By

Justine Amanda Burd, B.S.

Fairbanks, AK

May 2016

Abstract

Reactive halogen radicals (e.g. Br, Cl and their oxide forms) dominate tropospheric oxidation mechanisms during Arctic springtime (Feb. – Apr.) by depleting ozone and changing the fate of pollutants. During ozone depletion events, reactive bromine radicals rapidly oxidize mercury which gets subsequently deposited, becoming more bioavailable. During Arctic springtime, a heterogeneous surface reaction (referred to as BrO recycling) between hypobromous acid (HOBr) and bromide (Br^-) rapidly increases the abundance of reactive bromine episodically up to 40 pptv peaks. However, as spring transitions to summer (May - June), elevated reactive bromine levels suddenly decrease. There are two key requirements to maintain BrO recycling including surface area and sea salt (i.e. bromide) abundance. This study investigated environmental factors that impact BrO recycling during late spring (May-June) in the Arctic, including temperature, snowpack depth and rain/snow precipitation events. Near horizon BrO was measured using Multi-AXis Differential Optical Absorption Spectroscopy (MAX-DOAS) at Barrow, AK and above frozen Arctic sea ice. The late spring “end” to elevated reactive bromine (referred as the Seasonal End Date, SED) was objectively determined at all sites ($N=12$). Air temperature-derived melt onset dates were determined for all sites ($N=12$) and occurred within two days of the SED ($RMS = 1.8$ days, $R^2 = 0.989$). Through these studies, we determined BrO recycling is hindered by melt onset of snowpack, ending the reactive bromine season.

Table of Contents

	Page
Signature Page	i
Title Page	iii
Abstract	v
Table of Contents	vii
List of Figures	xi
List of Tables	xiii
Chapter 1: Introduction	1
1.1 Motivation.....	1
1.2 Arctic Tropospheric Chemistry.....	1
1.3 Bromine Explosion Mechanism.....	2
1.3.1 Saline Surfaces.....	3
1.3.2 Snow Surface Area	5
1.4 Melt Onset.....	6
1.5 Ion Pulse.....	7
1.6 Gas-Phase Bromine Seasonal Behavior.....	8
1.7 Multi-AXis Differential Optical Absorption Spectroscopy (MAX-DOAS).....	9
1.8 Thesis Structure	9
1.9 References.....	11
1.10 Figures.....	16

Chapter 2: Late Spring Snow Melt Onset Hinders Bromine Monoxide Heterogeneous

Recycling in the Arctic.....	17
2.1 Introduction.....	18
2.2 Data Sources and Methods.....	22
2.2.1 Bromine Monoxide Measurement Sites	22
2.2.2 Snow/ Rain Precipitation Observations and Snow Depth Measurements	23
2.2.3 Objective Determination of Seasonal End and Recurrence Events..	23
2.2.4 Objective Determination of Melt Onset Dates Using Surface Air Temperature	25
2.3 Results.....	26
2.3.1 Seasonal End Date Determination and Sensitivity to Threshold Parameters.....	26
2.3.2 Melt Onset Determination and Correlation to the Seasonal End Date	26
2.3.3 Snow Depth Changes at Seasonal End and Recurrence Events	28
2.3.4 Rain/Snow Precipitation at Seasonal End and Recurrence Events...	28
2.4 Discussion.....	29
2.4.1 Seasonal End Date is the Melt Onset Date	29
2.4.2 Decaying Snowpack and Rain Precipitation Prevents BrO Recycling	31

	Page
2.4.3 Below Freezing Temperatures and New Surface Area Re-initialize	
BrO Recycling	32
2.5 Conclusion	34
2.6 Acknowledgements.....	35
2.7 References.....	36
2.8 Figures.....	41
Chapter 3: Conclusions and Outlook	49
3.1 Conclusions.....	49
3.2 Future Outlook.....	50
3.3 References.....	52

List of Figures

	Page
Figure 1.1: Simplified bromine explosion cycle highlighting the surface heterogeneous reaction (i.e. BrO recycling) between hypobromous acid (HOBr) and bromide (Br ⁻).....	16
Figure 2.1: Pan-Arctic map of study site locations.....	41
Figure 2.2: Sea Ice (panel a, O-Buoy 11-2015) and coastal (panel b, Barrow 2014) case study sites that represent the typical relationship between BrO (top subplot) and temperature (bottom subplot) during late spring (May – June).....	42
Figure 2.3: Linear regression analysis of the seasonal end date (SED) and melt onset date (MOD).....	43
Figure 2.4: Histogram of the difference between the melt onset date (MO) and seasonal end date (SED).....	44
Figure 2.5: BrO 2° elevation angle dSCD (top subplot) and snow depth (bottom subplot) for for three separate O-Buoys and co-located ice-mass balance buoys (IMBs) (panel a, b/c, and d).....	45
Figure 2.6: Rain and snow precipitation events at Barrow, AK for 2009 (panel a), 2012 (panel b), 2013 (panel c) and 2014 (panel d).....	46

List of Tables

	Page
Table 2.1: Seasonal, recurrence and melt onset dates for all sites and years.....	47
Table 2.2: Noise threshold values and seasonal end date (SED) sensitivity test results for all sites and years.	48

1.1 Motivation

The Arctic's temperature has slowly increased over the past few decades (Hinzman et al., 2005; Serreze et al., 2000), resulting in a decrease in Arctic sea ice cover (Comiso et al., 2008) and shift of sea ice type (Comiso, 2012). Measurements of sea ice type since the 1980s has revealed a shift from multi-year sea ice (2-7 years old) to a more saline, seasonal first-year ice (<1 years old, ice that re-grows each year, Comiso, 2012). First-year ice regions produce higher reactive halogen levels than multi-year ice (Wagner et al., 2001) and a shift to a first-year ice-dominated climate could result in stronger ozone depletion events in March (Oltmans et al., 2012). In addition, trends in the summer season, melt onset to last day of melt, revealed it has lengthened by ~8 days per decade at Barrow (Stone, 2002) and ~5 days per decade for the Pan-Arctic region (Markus et al., 2009). A longer summer season results in a shorter winter and spring season when reactive halogen radicals (Cl, Br, and I radicals, and their oxide form ClO, BrO, and IO) are abundant. A future Arctic with a shorter winter and spring season, which would reduce the amount of time BrO is present, and more first-year ice present, stronger BrO presence, could have a cancelling effect on each other. Understanding environmental influences on reactive bromine production could give an indication of how reactive bromine will respond to future climate changes.

1.2 Arctic Tropospheric Chemistry

Tropospheric ozone is known to cause respiratory problems in humans and damage crops (McKee, 1994); however, in the Arctic, ozone provides critical oxidizing radicals to the troposphere, such as the hydroxyl radical (OH), and naturally dominates oxidation mechanisms of the troposphere (Platt and Hönninger, 2003; Simpson et al., 2007b, 2015). During Arctic

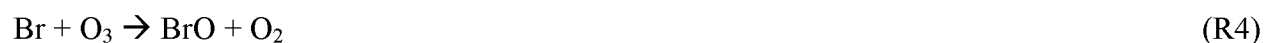
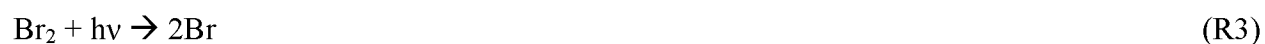
springtime, however, elevated levels of BrO are observed episodically up to 40 pptv (Hönninger and Platt, 2002; Pöhler et al., 2010). Elevated BrO levels are the result of ozone depletion events where reactive bromine radicals consume ozone to produce BrO as part of the *bromine explosion* cycle (see Section 1.3) and dominates the troposphere oxidation, discussed in section 1.3. During ozone depletion events, when ozone is near zero, reactive bromine radicals shift to rapidly oxidizing elemental mercury (Hg^0) to gaseous reactive mercury (Hg^{2+}), gaseous reactive mercury then gets subsequently deposited out of the troposphere and becomes more bioavailable (Holmes et al., 2006; Steffen et al., 2008). Future climatic changes with a first-year ice-dominated Arctic and stronger ozone depletion events during March (Oltmans et al., 2012), may induce a higher deposition of mercury.

1.3 Bromine Explosion Mechanism

The main source of BrO in the Arctic is from bromide (Br^-), an inactive species of bromine, present in sea salt or brine found on various surfaces. Bromide reacts to form BrO through the multi-step *bromine explosion* mechanism (Platt and Janssen, 1995). There are numerous additional chemical mechanisms that contribute to the bromine explosion cycle; however, this study focused on the main cycle that involves the surface heterogeneous reaction and will refer to this heterogeneous reaction as BrO recycling.

The bromine explosion cycle, as shown in R1-R4 and Figure 1.1, starts with the reaction between BrO and a hydroperoxy radical (HO_2), both of which come from wintertime chemistry and have been discussed as a “seed” to this mechanism, to produce hypobromous acid (HOBr, R1, Simpson et al., 2015). Hypobromous acid is a slightly acidic molecule and will adsorb to surfaces and heterogeneously react (i.e. BrO recycling) with bromide to produce gas-phase photolabile

bromine (Br_2 , R2). Photolabile bromine is a brown vapor and after polar sunrise quickly photolyzes to produce two reactive bromine radicals (Br , R3). Both reactive bromine radicals consume ozone (O_3) and produce two BrO radicals (R4). The BrO radical pool doubles per every one bromine explosion cycle completion.



To maintain rapid BrO recycling and elevated BrO levels, there are two critical requirements: high surface area and sea salt (i.e. bromide) availability. Changes to these critical requirements could hinder BrO recycling, breaking down the bromine explosion cycle and effectively decreasing BrO levels.

1.3.1 Saline Surfaces

Numerous surfaces and substrates in the Arctic have been proposed as areas where bromine activation can occur, including seawater, sea ice, frost flowers, sea salt aerosols and surface and blowing salt-contaminated snow (refer to the thorough review by Abbatt et al. (2012) and the references therein). Seawater has very low surface area and is known to only produce 1-3 pptv of BrO over open ocean (Leser et al., 2003). Seawater is rarely available as a surface during late spring due to the winter ice cover, although frequent sea ice leads could expose some seawater. Frost flowers were believed to produce elevated BrO (Rankin et al., 2002); however, it was found

that elevated BrO airmasses came in contact with first year ice areas more than potential frost flower areas (Simpson et al., 2007a). In addition, frost flower pH is buffered by the high salinity which makes it a less likely surface for BrO recycling (Huff and Abbatt, 2002). Snow and sea salt aerosols have been proposed as the predominant surfaces for BrO recycling due to their high surface area, bromide availability and more acidic pH.

Morin et al. (2008) proposed a process that BrO recycling is occurring in the interstitial space between snow grains. This was supported by Pratt et al. (2013) where they found Br₂, the product of BrO recycling, was detected only when surface snow (top 1 cm), above first-year ice and tundra, was exposed to sunlight and ozone. They conducted snow chamber experiments where various field snow and ice samples were examined for the production of Br₂. Snow and ice samples included surface snow (top 1 cm) above tundra, as well as basal snow (0-8 cm), sintered snow (8 – 18 cm), and surface snow (top 1 cm) above first year sea ice. In addition, a sea ice sample was cut out and put into the chamber. They found that only surface snow above both tundra and sea ice produced Br₂, the sintered layer produced Br₂ but only at high concentrations of ozone and the basal layer did not produce any Br₂. They found top 1 cm snow had more acidic pH as compared to the deeper layers, as well as a higher Br/Cl ratio. The authors discussed the dependence of pH as a control for Br₂ production. Surfaces with a high salt content shifts to a more alkaline pH, closer to that of seawater; whereas, surfaces with less salt and more exposure to aerosol deposition are more acidic. The pH dependence for Br₂ production has also been studied in the laboratory. Huff and Abbatt (2002) found that there was a higher uptake of HOBr and more production of Br₂ on frozen halide surfaces with a pH of 2, rather than surfaces with a pH of 6. Based on previous studies, pH seems to contribute towards the production of Br₂; however, more research is needed

to determine how much bromide is needed at the surface to maintain rapid BrO recycling. In addition to snow surfaces, aerosols have been proposed as a BrO recycling surface.

BrO recycling on aerosols was first proposed to occur on highly concentrated sulfuric acid aerosols by Fan and Jacob (1992), based on the observations of the high abundance of sulfate aerosols during ozone depletion events (Bottenheim et al., 1990). Later research proposed production of BrO through sea salt aerosols (Mozurkewich, 1995). Frieß et al. (2011) observed high aerosol extinction was correlated with elevated BrO levels during periods where snow and ice particles would become airborne at wind speeds exceeding 5 m s^{-1} . In addition, back trajectories of wind direction found that airmasses came in contact with first year ice areas and/or potential frost flowers. Therefore, it was suggested that ice particles or sea salt aerosols become airborne and are transported to the measurement site where reactive bromine is subsequently released (Frieß et al., 2011). More recently, a study found no clear relationship between aerosol particle extinction and wind speed, in which the authors suggest that blowing snow is not the sole contributor of aerosol particles aloft, needed for BrO recycling (Peterson et al., 2014).

1.3.2 Snow Surface Area

Snowpack has very high surface area, triple that of typical Earth surfaces, such as terrestrial soil (Dominé et al. 2002). Specific surface area (SSA) is a common measurement of snow grains and particles and is defined as the surface area of the air-ice interface per unit mass. SSA has been measured for a variety of snow types, including fresh dendritic crystals ($\text{SSA}=156 \text{ m}^2 \text{ kg}^{-1}$, Dominé et al., 2007) and diamond dust crystals ($\text{SSA} = 223 \text{ m}^2 \text{ kg}^{-1}$, Dominé et al., 2011). Analysis of the SSA of snowpack layers found the top 1 cm of the snowpack to have some of the highest SSA, around $40 - 150 \text{ m}^2 \text{ kg}^{-1}$, compared to deeper snowpack layers (Dominé et al., 2002). The SSA of

snowpack layers has also been observed to be anti-correlated with the layer density (Dominé et al., 2002; Gallet et al., 2014).

The surface area index, m^2 of snow per m^2 of Earth surface, of snowpack was additionally measured for both Arctic region and sub-Arctic regions. Dominé et al. (2002) were the first to describe the SAI (also known as total surface area, TSA) and found that Arctic snowpack has an SAI between 1160 to 3710 $\text{m}^2 \text{m}^{-2}$. Higher SAI came from snowpack with wind-packed layers. Sub-Arctic snowpack SAI averaged around 1000 $\text{m}^2 \text{m}^{-2}$ and the snowpack stratigraphy did not show as much wind-packed layers as seen in an Arctic snowpack (Taillandier et al., 2006).

As the snowpack experiences near freezing temperatures it goes through melt-freeze cycles and produces a melt crust at the top of the snowpack. This melt freeze crust has significantly lower SSA ($2 \text{ m}^2 \text{ kg}^{-1}$, Dominé et al., 2007) as compared to other snowpack layers.

1.4 Melt Onset

Various studies have examined melt onset in the Arctic (Anderson, 1987; Kwok et al., 2003; Markus et al., 2009; Winebrenner et al., 1994). Synthetic Aperture Radar (SAR) imagery was used to derive melt onset dates (Kwok et al., 2003). Melt onset dates were compared against both surface air temperatures and passive microwave brightness temperatures. Melt onset dates occurred within 1-2 days of the surface air temperature rising above 0°C . However, melt onset dates did not coincide with brightness temperatures indicating brightness temperatures are more sensitive to later stages of melt (Kwok et al., 2003). In addition, deployed buoy temperature records (International Arctic Buoy Project/POLar Exchange at the Sea Surface, IABP/POLES) were compared against passive-microwave-satellite-derived melt onset dates in the Arctic (Markus et al., 2009). The beginning of the maximum melt season, which coincided with the early melt onset

date, was defined as the first day the temperature reached freezing, regardless if it remained above freezing, and initiated melt-freeze cycles (Markus et al., 2009). At the onset of melt, snowpack starts to rapidly metamorphosize and the characteristics begin to change.

At the initiation of snowpack melting the SAI rapidly decreases from $3000 \text{ m}^2 \text{ m}^{-2}$ to $500 \text{ m}^2 \text{ m}^{-2}$ and continues to decrease until the snowpack is gone (Dominé et al., 2002; Taillandier et al., 2006). The rapid decrease in SAI at melt onset is due to snow grains starting to coalesce. As the liquid water content increases, larger snow grains form and round out (Brun, 1989). The clustering of grains can start to compact the snowpack. Melt-freeze cycles, re-freezing of melted snowpack due to temperature fluctuations, of the snowpack create a hard crust at the top of the snowpack that decreases its permeability and ventilation (Albert and Perron, 2000). Permeability of melt-freeze crusts 1-3 mm thick ranged from $1 - 19 \times 10^{-10} \text{ m}^2$ (permeability, K , is calculated based on the proportionality between pressure and flow rate through a porous medium); however, as air temperature increased the permeability nearly doubled to $44 \times 10^{-10} \text{ m}^2$ at 2°C . Permeability again doubled to $120 \times 10^{-10} \text{ m}^2$ when the temperature reached 10°C . This increase in permeability was in conjunction with melting, larger snow grain size and albedo decrease. Although permeability increased with melting, which would allow for more ventilation, the induction of melt would decrease the surface area with larger grain sizes, as well as elute ions from the snow grain surface that would be needed to maintain BrO recycling.

1.5 Ion Pulse

The ionic pulse phenomenon has been discussed as the surge of ions from the top or within the snowpack in the first snowmelt runoff of the season (Johannessen and Henriksen, 1978). Bales et al. (1989) found that chemical species at the top of the snowpack elute out well before species

distributed throughout the snowpack. They also found that 80% of salts at the top and 70% at mid-depth of the snowpack were removed with the first 20% of melt water. Bales et al. (1989) and Colbeck (1981) also discussed that melt-freeze cycles could induce rapid removal of ions due the decrease in specific surface area of the ice phase which creates a more porous snowpack and allows for liquid water to percolate through the snowpack.

1.6 Gas-Phase Bromine Seasonal Behavior

The earliest known study to look at the seasonality of atmospheric bromine was Berg et al. (1983) who measured particulate bromine in Arctic aerosols at Barrow, AK from 1976-1980. They found a seasonal maximum of particulate bromine from February – May of each year and as June approached there was a rapid decrease in the amount of particulate bromine present. Although it is still under question exactly which bromine species they were observing, the seasonality of bromine in their results are similar to the results presented in this thesis.

The seasonality of BrO has also been observed by satellite over the pan-Arctic region. Elevated BrO columns were observed over the pan-Arctic region through the GOME ERS-2 satellite in the spring and summer of 1997 (Richter et al., 1998; Wagner and Platt, 1998). Richter et al. (1998) found large, persistent elevated BrO columns over the Hudson Bay and Canadian Arctic areas and smaller events were reported over the coast line of the Arctic Sea and polar ice. These large and smaller events occurred between early February through the end of May and Richter et al. (1998) discussed that there was no evidence of elevated BrO after the middle of June. Wagner and Platt (1998) reported similar results; however, they specifically found BrO was elevated near or over areas of frozen salt water.

1.7 Multi-AXis Differential Optical Absorption Spectroscopy (MAX-DOAS)

The most widely used instrument that measures BrO, and additional trace gases, is differential optical absorption spectrometry (DOAS). The DOAS technique uses sunlight scattering to quantify trace gas abundance using narrow band absorption wavelengths in the UV and visible region (Hönninger et al., 2004). The Multi-AXis DOAS is a passive instrument that requires sunlight and quantifies trace gases through multiple viewing elevations (2°, 5°, 10°, 20°); therefore, it is more sensitive to boundary layer gases due to its near-horizon view (Hönninger et al., 2004; Carlson et al., 2010). The MAX-DOAS is a simple and lightweight instrument, with low power consumption, which makes it a useful option for field campaigns. Although the MAX-DOAS is useful to measure boundary layer gases, there are two main disadvantages to this instrument. First, it relies on scattered sunlight; therefore, measurements can only be taken during the day or at twilight. Second, converting from differential slant column densities (dSCD) to concentrations or mixing ratios can be an intensive process and sometimes all the data needed to convert over is not available. Overall the MAX-DOAS is a good option for remote field campaigns due to its light, compact set up and low power consumption abilities; however, it has a couple drawbacks to its measurement techniques.

1.8 Thesis Structure

This work begins with background information in Chapter 1 regarding the rapid recycling of reactive bromine species through the *bromine explosion* cycle and the contribution of saline surfaces and surface area in maintaining this cycle. Chapter 1 ends with the discussion of the changes, upon snowmelt, in surface area and/or salinity of surfaces that could hinder BrO recycling. Chapter 2 presents evidence that melt onset hinders BrO recycling and ends the reactive

bromine season. Snowpack surface area loss due to the increase of snow grain size and compaction of the snowpack are discussed. In addition, ions re-distributing down the snowpack, due to an ion pulse, around the time of the seasonal end of BrO is discussed. This work has been prepared for submission to the *Atmospheric Chemistry and Physics* journal. Thesis conclusions and future outlooks are summarized in Chapter 3.

1.9 References

- Abbatt, J. P. D., Thomas, J. L., Abrahamsson, K., Boxe, C., Granfors, A., Jones, A. E., King, M. D., Saiz-Lopez, A., Shepson, P. B., Sodeau, J., Toohey, D. W., Toubin, C., von Glasow, R., Wren, S. N. and Yang, X.: Halogen activation via interactions with environmental ice and snow in the polar lower troposphere and other regions, *Atmos. Chem. Phys.*, 12(14), 6237–6271, doi:10.5194/acp-12-6237-2012, 2012.
- Albert, M. R. and Perron, F. R.: Ice layer and surface crust permeability in a seasonal snow pack, *Hydrol. Process.*, 14(September), 3207–3214, 2000.
- Anderson, M. R.: The Onset of Spring Melt in First-Year Ice Regions of the Arctic as Determined From Scanning Multichannel Microwave Radiometer Data for 1979 and 1980, *J. Geophys. Res.*, 92(13), 153 – 163, 1987.
- Bales, R. C., Davis, R. E. and Stanley, D. A.: Ion elution through shallow homogeneous snow, *Water Resour. Res.*, 25(8), 1869–1877, doi:10.1029/WR025i008p01869, 1989.
- Berg, W. W., Sperry, P. D., Rahn, K. A. and Gladney, E. S.: Atmospheric Bromine in the Arctic, *J. Geophys. Res.*, 88(3), 6719–6736, doi:10.1029/JC088iC11p06719, 1983.
- Bottenheim, J. W., Barrie, L. A., Atlas, E., Heidt, L. E., Niki, H., Rasmussen, R. A. and Shepson, P. B.: Depletion of lower tropospheric ozone during Arctic spring: The Polar Sunrise Experiment 1988, *J. Geophys. Res.*, 95(D11), 18555, doi:10.1029/JD095iD11p18555, 1990.
- Brun, E.: Investigation on wet-snow metamorphism in respect of liquid-water content, *Ann. Glaciol.*, 13, 22–26, 1989.
- Carlson, D., Donohue, D., Platt, U. and Simpson, W. R.: A low power automated MAX-DOAS instrument for the Arctic and other remote unmanned locations, *Atmos. Meas. Tech.*, 3(5), 2347–2375, 2010.
- Colbeck, S. C.: A Simulation of the Enrichment of Atmospheric Pollutants, *Water Resour. Res.*, 17(5), 1383–1388, 1981.
- Comiso, J. C.: Large decadal decline of the arctic multiyear ice cover, *J. Clim.*, 25(4), 1176–1193, doi:10.1175/JCLI-D-11-00113.1, 2012.
- Comiso, J. C., Parkinson, C. L., Gersten, R. and Stock, L.: Accelerated decline in the Arctic sea ice cover, *Geophys. Res. Lett.*, 35(1), 1–6, doi:10.1029/2007GL031972, 2008.

- Dominé, F., Taillandier, A. S. and Simpson, W. R.: A parameterization of the specific surface area of seasonal snow for field use and for models of snowpack evolution, *J. Geophys. Res. Earth Surf.*, 112(2), 1–13, doi:10.1029/2006JF000512, 2007.
- Dominé, F., Gallet, J. C., Barret, M., Houdier, S., Voisin, D., Douglas, T. A., Blum, J. D., Beine, H. J., Anastasio, C. and Breon, F. M.: The specific surface area and chemical composition of diamond dust near Barrow, Alaska, *J. Geophys. Res. Atmos.*, 116(23), 1–18, doi:10.1029/2011JD016162, 2011.
- Dominé, F., Cabanes, A. and Legagneux, L.: Structure, microphysics, and surface area of the Arctic snowpack near Alert during the ALERT 2000 campaign, *Atmos. Environ.*, 36(15-16), 2753–2765, doi:10.1016/S1352-2310(02)00108-5, 2002.
- Fan, S. M. and Jacob, D. J.: Surface ozone depletion in Arctic spring sustained by bromine reactions on aerosols, *Lett. to Nat.*, 359, 522–524, 1992.
- Frieß, U., Sihler, H., Sander, R., Phler, D., Yilmaz, S. and Platt, U.: The vertical distribution of BrO and aerosols in the Arctic: Measurements by active and passive differential optical absorption spectroscopy, *J. Geophys. Res. Atmos.*, 116(18), 1–19, doi:10.1029/2011JD015938, 2011.
- Gallet, J. C., Dominé, F., Savarino, J., Dumont, M. and Brun, E.: The growth of sublimation crystals and surface hoar on the Antarctic plateau, *Cryosphere*, 8(4), 1205–1215, doi:10.5194/tc-8-1205-2014, 2014.
- Hinzman, L. D., Bettez, N. D., Bolton, W. R., Chapin, F. S., Dyurgerov, M. B., Fastie, C. L., Griffith, B., Hollister, R. D., Hope, A., Huntington, H. P., Jensen, A. M., Jia, G. J., Jorgenson, T., Kane, D. L., Klein, D. R., Kofinas, G., Lynch, A. H., Lloyd, A. H., McGuire, A. D., Nelson, F. E., Oechel, W. C., Osterkamp, T. E., Racine, C. H., Romanovsky, V. E., Stone, R. S., Stow, D. A., Sturm, M., Tweedie, C. E., Vourlitis, G. L., Walker, M. D., Walker, D. A., Webber, P. J., Welker, J. M., Winker, K. S. and Yoshikawa, K.: Evidence and implications of recent climate change in Northern Alaska and other Arctic regions, *Clim. Change*, 72(3), 251–298, doi:10.1007/s10584-005-5352-2, 2005.
- Holmes, C. D., Jacob, D. J. and Yang, X.: Global lifetime of elemental mercury against oxidation by atomic bromine in the free troposphere, *Geophys. Res. Lett.*, 33(20), 1–5, doi:10.1029/2006GL027176, 2006.
- Hönninger, G., von Friedeburg, C. and Platt, U.: Multi axis differential optical absorption spectroscopy (MAX-DOAS), *Atmos. Chem. Phys.*, 4, 231–254, 2004.

- Hönninger, G. and Platt, U.: Observations of BrO and its vertical distribution during surface ozone depletion at Alert, *Atmos. Environ.*, 36(15-16), 2481–2489, doi:10.1016/S1352-2310(02)00104-8, 2002.
- Huff, A. K. and Abbatt, J. P. D.: Kinetics and product yields in the heterogeneous reactions of HOBr with ice surfaces containing NaBr and NaCl, *J. Phys. Chem. A*, 106(21), 5279–5287, doi:10.1021/jp014296m, 2002.
- Johannessen, M. and Henriksen, A.: Chemistry of snow melt water: changes in concentration during melting, *Water Resour. Res.*, 14(4), 615–619, 1978.
- Kwok, R., Cunningham, G. F. and Nghiem, S. V.: A study of the onset of melt over the Arctic Ocean in RADARSAT synthetic aperture radar data, *J. Geophys. Res. Ocean.*, 108(C11), 3363, doi:10.1029/2002JC001363, 2003.
- Leser, H., Hönninger, G. and Platt, U.: MAX-DOAS measurements of BrO and NO₂ in the Marine Boundary Layer, *Geophys. Res. Lett.*, 30(10), 3–6, doi:10.1029/2002GL015811, 2003.
- Markus, T., Stroeve, J. C. and Miller, J.: Recent changes in Arctic sea ice melt onset, freezeup, and melt season length, *J. Geophys. Res. Ocean.*, 114(12), 1–14, doi:10.1029/2009JC005436, 2009.
- McKee, D., Ed.: *Tropospheric Ozone: Human Health and Agricultural Impacts*, Lewis Publishers., 1994.
- Morin, S., Marion, G. M., von Glasow, R., Voisin, D., Bouchez, J. and Savarino, J.: Precipitation of salts in freezing seawater and ozone depletion events: a status report, *Atmos. Chem. Phys.*, 8(3), 7317–7324, doi:10.5194/acpd-8-9035-2008, 2008.
- Mozurkewich, M.: Mechanisms for the release of halogens from sea-salt particles by free radical reactions, *J. Geophys. Res.*, 101(D 4), 9121–9138, 1995.
- Oltmans, S. J., Johnson, B. J. and Harris, J. M.: Springtime boundary layer ozone depletion at Barrow, Alaska: Meteorological influence, year-to-year variation, and long-term change, *J. Geophys. Res. Atmos.*, 117(8), 1–18, doi:10.1029/2011JD016889, 2012.
- Peterson, P. K., Simpson, W. R., Pratt, K. A., Shepson, P. B., Frieß, U., Zielcke, J., Platt, U., Walsh, S. J. and Nghiem, S. V.: Meteorological controls on the vertical distribution of bromine monoxide in the lower troposphere, *Atmos. Chem. Phys. Discuss.*, 14(17), 23949–23994, doi:10.5194/acpd-14-23949-2014, 2014.

- Platt, U. and Hönninger, G.: The role of halogen species in the troposphere., *Chemosphere*, 52(2), 325–38, doi:10.1016/S0045-6535(03)00216-9, 2003.
- Platt, U. and Janssen, C.: Observation and role of the free radicals NO₃, ClO, BrO and IO in the troposphere, *Faraday Discuss.*, 100, 175, doi:10.1039/fd9950000175, 1995.
- Pöhler, D., Vogel, L., Friess, U. and Platt, U.: Observation of halogen species in the Amundsen Gulf, Arctic, by active long-path differential optical absorption spectroscopy., *Proc. Natl. Acad. Sci. U. S. A.*, 107(15), 6582–6587, doi:10.1073/pnas.0912231107, 2010.
- Pratt, K. A., Custard, K. D., Shepson, P. B., Douglas, T. A., Pöhler, D., General, S., Zielcke, J., Simpson, W. R., Platt, U., Tanner, D. J., Gregory Huey, L., Carlsen, M. and Stirm, B. H.: Photochemical production of molecular bromine in Arctic surface snowpacks, *Nat. Geosci.*, 6(5), 351–356, doi:10.1038/ngeo1779, 2013.
- Rankin, A. M., Wolff, E. W. and Martin, S.: Frost flowers: Implications for tropospheric chemistry and ice core interpretation, *J. Geophys. Res. Atmos.*, 107(23), doi:10.1029/2002JD002492, 2002.
- Richter, A., Wittrock, F., Eisinger, M. and Burrows, J. P.: GOME Observations of Tropospheric BrO in Northern Hemispheric Spring and Summer 1997, *Geophys. Res. Lett.*, 25(14), 2683–2686, 1998.
- Serreze, M. C., Walsh, J.E., Chapin III, F. S., Osterkamp, T., Dyurgerov, M., Romanovsky, V., Oechel, W. C., Morison, J., Zhang, T. and Barry, R. G.: Observational evidence of recent change in the northern high latitude environment, *Clim. Change*, 46, 159–207, 2000.
- Simpson, W. R., Carlson, D., Hönninger, G., Douglas, T. A., Sturm, M., Perovich, D. and Platt, U.: First-year sea-ice contact predicts bromine monoxide (BrO) levels at Barrow, Alaska better than potential frost flower contact, *Atmos. Chem. Phys.*, 7(3), 621–627, doi:10.5194/acp-7-621-2007, 2007a.
- Simpson, W. R., von Glasow, R., Riedel, K., Anderson, P., Ariya, P., Bottenheim, J., Burrows, J., Carpenter, L., Frieß, U., Goodsite, M. E., Heard, D., Hutterli, M., Jacobi, H. W., Kaleschke, L., Neff, B., Plane, J., Platt, U., Richter, A., Roscoe, H., Sander, R., Shepson, P., Sodeau, J., Steffen, A., Wagner, T. and Wolff, E.: Halogens and their role in polar boundary-layer ozone depletion, *Atmos. Chem. Phys.*, 7(2), 4375–4418, doi:10.5194/acpd-7-4285-2007, 2007b.
- Simpson, W. R., Brown, S. S., Saiz-Lopez, A., Thornton, J. A. and Glasow, R. Von: Tropospheric Halogen Chemistry: Sources, Cycling, and Impacts, *Chem. Rev.*, 150312153236002, doi:10.1021/cr5006638, 2015.

- Steffen, A., Douglas, T., Amyot, M., Ariya, P., Aspmo, K., Berg, T., Bottenheim, J., Brooks, S., Cobbett, F., Dastoor, A., Dommergue, A., Ebinghaus, R., Ferrari, C., Gardfeldt, K., Goodsite, M. E., Lean, D., Poulain, A. J., Scherz, C., Skov, H., Sommar, J. and Temme, C.: A synthesis of atmospheric mercury depletion event chemistry in the atmosphere and snow, *Atmos. Chem. Phys.*, 8(6), 1445–1482, doi:10.5194/acp-8-1445-2008, 2008.
- Stone, R. S.: Earlier spring snowmelt in northern Alaska as an indicator of climate change, *J. Geophys. Res.*, 107(D10), doi:10.1029/2000JD000286, 2002.
- Taillandier, A. S., Dominé, F., Simpson, W. R., Sturm, M., Douglas, T. A. and Severin, K.: Evolution of the snow area index of the subarctic snowpack in central Alaska over a whole season. Consequences for the air to snow transfer of pollutants, *Environ. Sci. Technol.*, 40(24), 7521–7527, doi:10.1021/es060842j, 2006.
- Wagner, T. and Platt, U.: Satellite mapping of enhanced BrO concentrations in the troposphere, *Nature*, 395(October), 486–490, doi:10.1038/26723, 1998.
- Wagner, T., Leue, C., Wenig, M., Pfeilsticker, K. and Platt, U.: Spatial and temporal distribution of enhanced boundary layer BrO concentrations measured by the GOME instrument aboard ERS-2, *J. Geophys. Res.*, 106(D20), 24225, doi:10.1029/2000JD000201, 2001.
- Winebrenner, D. P., Nelson, E. D., Colony, R. and West, R. D.: Observation of melt onset on multiyear Arctic sea ice using the ERS 1 synthetic aperture radar, *J. Geophys. Res.*, 99(C11), 22,425–22,441, doi:10.1029/94JC01268, 1994.

1.10 Figures

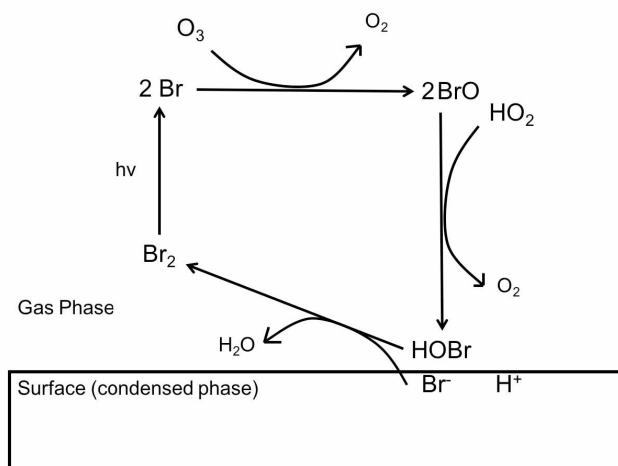


Figure 1.1: Simplified bromine explosion cycle highlighting the surface heterogeneous reaction (i.e. BrO recycling) between hypobromous acid (HOBr) and bromide (Br^-).

Chapter 2: Late Spring Snow Melt Onset Hinders Bromine Monoxide Heterogeneous
Recycling in the Arctic¹

Reactive bromine radicals deplete ozone and alter tropospheric oxidation mechanisms during the Arctic springtime (Feb. – Mar.). Elevated bromine monoxide (BrO) levels are routinely measured during Arctic spring and can reach up to 40 pptv during the day. However, as spring transitions to summer (May – Jun.) elevated BrO levels rapidly decrease. This late spring transition is also associated with above freezing air temperatures which initiates snow melt. Bromine monoxide differential slant column densities (dSCD) at near-horizon (2° elevation), an indication of boundary layer BrO abundance, was measured by Multi-AXis Differential Optical Absorption Spectrometer (MAX-DOAS) at Barrow, AK from 2008-2014 and on drifting buoys deployed in Arctic sea ice from 2011-2015. The seasonal end date (SED) of elevated BrO was objectively determined for all sites and years ($N=12$) and compared to surface-air-temperature-derived melt onset dates during late spring (May-Jun.). The seasonal end date of elevated BrO occurred within 2 days of the melt onset date in all cases ($N=12$, $R^2 = 0.989$, $RMS = 1.8$ days). In a subset of these sites/years where ancillary data was available, we observed that snowpack depth decay ($N=4$) and rain precipitation ($N=4$) occurred within one day of the SED. Taken in total, the results of this study suggests the onset of snowpack melt hinders elevated BrO production. With a projected warmer Arctic, and a shift to earlier snow melt seasons, snow melt periods are likely to be initiated

¹ Burd, J.A., Peterson, P.K., Nghiem, S.V., and Simpson, W.R.: Late Spring Snow Melt Onset Hinders Bromine Monoxide Heterogeneous Recycling in the Arctic, *Atmospheric Chemistry and Physics*, in preparation for submission in 2016.

earlier. This could drastically alter the timing and role of halogen chemical reactions in the Arctic with ramifications on ozone photochemistry and mercury deposition.

2.1 Introduction

Reactive bromine species (Br and its oxide form BrO) are strong tropospheric oxidizers (Platt and Hönninger, 2003; Simpson et al., 2007, 2015). During Arctic springtime (February – April), elevated BrO levels have been observed episodically up to 40 pptv (Hönninger and Platt, 2002; Pöhler et al., 2010) as compared to levels found in the marine boundary layer of 1-3 pptv (Leser et al., 2003). Ozone normally dominates tropospheric oxidation by providing reactive oxidizers, such as the hydroxyl radical (Hönninger and Platt, 2002); however, during springtime reactive bromine rapidly consumes ozone (ozone depletion events) and produces BrO (Bottenheim et al., 1990; Fan and Jacob, 1992; McConnell et al., 1992; Hausmann and Platt, 1994). In addition, during ozone depletion events, reactive bromine rapidly oxidizes mercury from Hg^0 to Hg^{2+} which gets subsequently deposited, becoming more bioavailable (Holmes et al., 2006; Steffen et al., 2008). As spring transitions to summer (i.e. late spring, May – June), however, observed BrO levels start to decrease and less ozone depletion events are observed.

Springtime in the Arctic is dominated by snowpack-covered sea ice and cold temperatures. However, during late spring the air temperature increases to above freezing and the snowpack starts to melt. In addition, elevated BrO levels suddenly decrease. We will refer to the spring to summer seasonal shift of BrO as BrO seasonality. BrO seasonality has been observed by satellites for the Pan-Arctic region through the measurement of BrO vertical column densities (VCD). Elevated BrO VCD ($6-10 \times 10^{13}$ molecules cm^{-2}) are observed between February and May (Richter et al., 1998; Wagner et al., 2001); however, BrO VCD is down to “background” levels of 1-3 x

10^{13} molecules cm^{-2} by June (Van Roozendaal et al., 2002). Ground based observations of particulate bromine in aerosols at Barrow, AK reported by Berg et al. (1983) showed elevated particulate bromine levels (average 82 pptm, mass bromine/mass of aerosol) from February to April with decreasing values in May and very low levels (6 pptm) in June. In addition to observing BrO seasonality, ozone depletion events can be used as a proxy for elevated BrO levels, due to the high correlation between BrO and ozone depletion events (Fan and Jacob, 1992; McConnell et al., 1992; Hönninger and Platt, 2002). Oltmans et al. (1989) measured seasonal surface ozone at Igloodik, Barrow, Mould Bay, and Alert. The average behavior of ozone at Barrow had a winter maximum (November – February), decreased episodically in springtime (March – mid-May), and a secondary maximum in June. This ozone seasonality and the strong anti-correlation with BrO infers that when ozone levels are low, BrO levels are high and vice versa. The BrO maximum observed in springtime is due to the *bromine explosion* mechanism (Platt and Janssen, 1995). Bromide, the inactive species of bromine, is found in sea salt and resides on surfaces such as frozen sea ice, frost flowers (vapor deposited crystalline structures), sea salt aerosols and snow throughout the Arctic (Abbatt et al., 2012). Bromide is activated to reactive bromine through a heterogeneous reaction with hypobromous acid (HOBr), we will refer to this heterogeneous reaction as BrO recycling. Two main requirements for BrO recycling are a high surface area to facilitate the reaction and sea salt as a halogen source (i.e. bromide).

Laboratory studies have observed the BrO recycling on halide doped frozen surfaces and found that more acidic surfaces were more efficient at producing Br_2 (Huff and Abbatt, 2002). This was verified by a snow-chamber field experiment by Pratt et al. (2013) with snow and ice samples collected ~5km inland and ~3km north of Barrow, AK. They found that only the top 1 cm of the snowpack above both sea ice and tundra produced Br_2 , when exposed to sunlight and ozone,

as compared to sea ice and deeper snowpack layers (0-18 cm above the sea ice surface). They found that the top 1 cm had a higher Br/Cl ratio, was more acidic (due to aerosol deposition) and had the most air-surface interactions. It was discussed by Pratt et al. (2013) that as the salinity of a surface increases, the pH becomes more alkaline which decreases the uptake of HOBr and Br₂ production. Although it is clear, based on laboratory and field studies, that a more acidic surface is needed for BrO recycling, it is still unclear how much bromide is necessary on surfaces to maintain the bromine explosion cycle and produce Arctic springtime BrO levels.

Multiple saline surfaces have been suggested to contribute towards BrO recycling, including snow, ice, and aerosols (Abbatt et al., 2012). Snow has been discussed as a predominant site for BrO recycling due to its high surface area. Measurements of Arctic snowpack surface area index (SAI, m² of snow per m² of ground) revealed the snowpack to have incredibly high surface area (up to 3000 m² m⁻², Dominé et al., 2002) compared to typical terrestrial soil. Dominé et al. (2002) classified snowpack layers and measured the SAI of each layer during the ALERT2000 campaign. SAI measurements of Arctic snowpack layers above land near the Alert Station and sea ice (near Joliffe Bay and Williams Island) revealed the top 1 cm of the snowpack to be generally surface hoar and/or diamond dust with an SAI ranging from 50 – 120 m² m⁻² and had lower total surface area compared to depth hoar (300 – 500 m² m⁻²) and wind-packed layers (1000 – 2500 m² m⁻²). The highest total surface area was measured in the wind-packed layers; however, these layers are very dense and less ventilated than surface and depth hoar layers (Albert and Shultz, 2002). Snowpack will naturally metamorphosize throughout winter, but as the season moves into late spring warmer temperatures and melting will initiate rapid snowpack metamorphosis.

At the onset of snowpack melt, there is a loss of surface area (Dominé et al., 2002) and elution of ions downward in a snowpack. Various studies have examined melt onset of snowpack

in the Arctic (Anderson, 1987; Winebrenner et al., 1994; Kwok et al., 2003; Markus et al., 2009;). Kwok et al. (2003) derived melt onset dates by Satellite Aperture Radar (SAR) satellite imagery and compared the melt onset dates against individual buoy temperature measurements (International Arctic Buoy Program, IABP), as well as passive microwave brightness temperatures. They reported that melt onset occurred within 1-2 days of the buoy temperature crossing over 0°C; however, the passive microwave brightness temperatures were biased towards a later melt stage. A portion of research by Markus et al. (2009) analyzed the minimum and maximum melt season length using the POLar Exchange at the Sea Surface (POLES) temperature data. The beginning of the maximum melt season, which coincided with the early melt onset date, was the first day the surface temperature increased to above freezing, independent of it staying above freezing. The onset of snow melt is a critical time for the snowpack because snow grains begin to coalesce and ionic species are eluted downwards. Previous research has found that ions and pollutants on the surface of snow grains are the first elute into melt waters. This “ionic pulse” phenomenon was first defined for macroscopic processes where 80% of ions in a snowpack eluted within the first 30% of snow melt water (Bales et al., 1989; Johannessen and Henriksen, 1978). Bales et al. (1989) conducted a cold room experiment where various ion tracers, including bromide, were misted at the top (0.4 cm) or mid-depth (10 cm) of the snowpack. They raised the cold room temperature to 0°C and induced snow pack melting by thermal radiation using a black aluminum plate. They concluded that ion species at the top of the snowpack were removed first, before the species at mid-depth. Based on the ion pulse phenomenon, bromide species would be removed from the top of the snowpack at the onset of melt and could, in turn, inhibit BrO recycling.

To understand how environmental conditions associated with the onset of the late spring melt period may affect BrO recycling we conducted this study. BrO differential slant column

densities (dSCDs) were retrieved using a Multi-AXis Differential Optical Absorption Spectrometer (MAX-DOAS, Hönninger et al., 2004). Bromine monoxide dSCDs were used in this study for all analyses. We used BrO dSCDs, rather than converting to concentration or mixing ratio, because it gave us a consistent measurement to monitor BrO behavior spatially and temporally. In addition, BrO dSCDs could not be converted due to missing information needed to estimate the path length, such as the azimuth angle. The aim the research was to investigate changing environmental factors during the spring to summer seasonal transition and determine the influence on BrO recycling. A key goal for this study was to determine the relationship between temperature and BrO and whether a temperature threshold could be established. We also investigated ancillary environmental factors, including snow depth and snow/rain precipitation, on snowpack crystal metamorphosis and elution processes that move reactive halogens from the surface to the base of the snowpack.

2.2 Data Sources and Methods

2.2.1 Bromine Monoxide Measurement Sites

One MAX-DOAS instrument was permanently placed at Barrow, AK (156.6679°W, 71.3249°N) from 2008 – 2009, and 2012 – 2015. MAX-DOAS instruments were also mounted on top O-Buoy instruments that were deployed into various locations above the frozen Arctic Ocean between 2009 – 2015. O-Buoy instruments and deployments were a part of the Network of Arctic Ocean Chemical Sensors project. O-Buoys were designed for year-round measurement of bromine monoxide, ozone and carbon dioxide, in addition to meteorological variables, such as temperature and wind (Carlson et al., 2010; Knepp et al., 2010). O-Buoy deployments started in 2009 and a total of 15 O-Buoys have been deployed over 6 years. Only a subset of deployed O-Buoys retrieved

BrO dSCD measurements over the time range needed (April-June) for this study. All Barrow and O-Buoy sites and years were placed into two categories based on their location criteria, “coastal” or “sea ice” sites. See Table 2.1 for a list of all sites and locations and Figure 2.1 for a map of all sites at the time of the seasonal end date.

2.2.2 Snow/ Rain Precipitation Observations and Snow Depth Measurements

Meteorological Terminal Aviation Routine Weather Reports (METAR) at Barrow Airport (PABR, 156.7922 °W, 71.2826 °N) were used to determine daily snow and/or rain precipitation. Hourly METAR were obtained from the Iowa Environmental Mesonet (IEM, <http://mesonet.agron.iastate.edu>). Snow depth was measured through Ice Mass Balance Buoys (IMB, Perovich et al., 2013). An acoustic sounder was mounted on a pole frozen into the the ice and positioned above the snow/ice surface. The acoustic sounder measured the distance between the instrument and the snow surface, with an accuracy of 5 mm, every hour. Snow depth was then calculated by subtracting the sea ice surface location (measured by a sea ice acoustic sounder) from the snow surface location. Six total IMBs were deployed with O-Buoys; however, only four IMBs had reliable sounder data that could be used for analysis (refer to Table 2.2 for co-located instruments).

2.2.3 Objective Determination of Seasonal End and Recurrence Events

Observations of BrO seasonality revealed a sudden decrease of BrO in late spring, referred to as the Seasonal End Date (SED). Figure 2.2 shows two typical examples of the SED, panel A and B. In panel A, the top subplot reveals elevated BrO ranging from $2-4 \times 10^{14}$ molecules cm^{-2} until May 18th, then on May 19th the BrO level dropped to between $0-1 \times 10^{14}$ molecules cm^{-2} for

about 5 days. This same behavior is seen in panel B where the the BrO levels dropped off suddenly on April 30th. Both case studies presented in Figure 2.2 also had periods where the BrO level recovered, after the SED, and is referred to as a recurrence event. Both the seasonal end and recurrence events gave us indication of the change in BrO behavior and we wanted to objectively determine these dates through an algorithm.

Our first approach to objectively determining the SED and recurrence events was to single out the 2° elevation BrO dSCDs from the data set because it is the most sensitive to boundary layer BrO abundance. Each BrO dSCD point has an associated noise error. At every site and year, a cumulative histogram was generated to determine the 90th percentile noise error threshold. BrO dSCD points with noise error greater than the noise error threshold were removed from the data set. The BrO dSCD points were smoothed by performing a 3-point running average to further reduce the influence of noise. Finally, using the smoothed data, our metric calculated the SED by determining the first day BrO dSCD dropped below 5×10^{13} molecules cm^{-2} (the BrO threshold) and remained below the BrO threshold for five consecutive days. At a few sites and years, recurrence events were determined when BrO recovered above the BrO threshold two or more consecutive days; the first day of the recurrence event is referred to as the Recurrence Start Date (RSD) and the last day is the Recurrence End Date (RED), which is calculated by the same “seasonal end date” algorithm described above.

Sensitivity tests were performed on the SED, RSD, and RED events to make sure small changes would not significantly change any of these events. Two tests were performed to test sensitivity, the BrO threshold and number of consecutive days were varied approximately $\pm 30\%$ in both tests.

ST1: The number of consecutive days was varied from 3-7 days in one-day increments, holding the BrO threshold (5×10^{13} molecules cm^{-2}) constant.

ST2: The BrO threshold was varied between 3.5×10^{13} molecules cm^{-2} and 6.5×10^{13} molecules cm^{-2} in 0.5×10^{13} molecules cm^{-2} increments while the number of consecutive days (5 days) remained constant.

2.2.4 Objective Determination of Melt Onset Dates Using Surface Air Temperature

Two meter, above ground level, air temperature at Barrow, AK was obtained from NOAA Earth System Research Laboratory Global Monitoring Division (<http://www.esrl.noaa.gov/gmd/dv/data/>). Air temperature measurements on the O-Buoy instruments were taken in conjunction with the BrO measurements and were obtained from the ACADIS website (www.aoncadis.org). The O-Buoy temperature sensor was roughly 2-3 meters above the sea ice, depending upon snow depth and ice melt condition.

Figure 2.2 shows two examples of the temperature relationship and BrO. In the bottom subplot of panel A, the temperature remained below freezing until the SED (black line) where the temperature raised to 0°C . The temperature generally hovered around 0°C after the SED; however, during the recurrence event the temperature dropped below 0°C throughout the recurrence event. Based on Markus et al. (2009) and Kwok et al. (2003) studies we defined the date the temperature reaches 0°C as the melt onset date. The melt onset date (MOD) for this study was determined using the maximum daily temperature (T_{max}). Melt onset dates were reported when the maximum temperature reached or exceeded freezing ($\text{MOD} = T_{\text{max}} \geq 0^{\circ}\text{C}$), independent of it remaining above freezing.

2.3 Results

2.3.1 Seasonal End Date Determination and Sensitivity to Threshold Parameters

The first reported SED for algorithm is displayed in Table 2.1. Early seasonal dates were reported at O-Buoy 1 (DOY 47) and 10 (DOY 106); however, it was determined these early season dates were a separate event from the SED and the second reported SED was used. Barrow 2008 had data collection issues for 3 days due to a frosted window at the time of the SED. Therefore, the SED was unreliable and Barrow 2008 was removed from the data analysis. Refer to Table 2.1 for all reported SEDs at each site and year, as well as recurrence dates. The ST1 and ST2 tests revealed the SED, RSD and RED have low sensitivity to changes in the BrO threshold and consecutive days (see Table 2.2 for sensitivity test results for the SED). The largest deviation between the reported dates was in the variation of the BrO threshold (ST1 test), later dates were reported if the BrO threshold was lowered and early dates were reported if the BrO threshold was raised, in most cases. Overall, the dates reported from the sensitivity tests generally fell within three days ($RMS = 3.2$ days) of the SED at 5×10^{13} molecules cm^{-2} BrO threshold and 5 consecutive days.

2.3.2 Melt Onset Determination and Correlation to the Seasonal End Date

Melt onset dates (MOD) were reported for all sites and years and can be found in Table 2.1. The first date reported by the algorithm for most sites and years ($N=9$) was considered the melt onset date. Early warming periods were observed at three sites and years (Barrow 2013, O-Buoy 6 2012 and O-Buoy 10-2014) where the temperature reached 0°C over 10 days prior to the SED. These early warming periods lasted between 1 to 3 days. O-Buoys 6 and 10-2014 experienced a couple warming periods prior to the SED whereas Barrow measurements 2013

reported only one early warming period. These early warming periods were also observed by Winebrenner et al. (1994). They detected snowpack melting using backscattering from the European Remote Sensing 1 (ERS 1) SAR satellite imagery. They reported that almost all melt onset occurred when the temperature reached 0°C; however, in one case they saw multiple periods where the temperature reached 0°C before the melt onset date. They referred to these periods as “false start” of melting and explained that these short periods “did not lead to irreversible physical changes in those ice and snow properties that control backscattering at 5.3 GHz.” A linear regression of the SED and early warming dates produced a poor R^2 value of 0.346; therefore, based on previous literature and poor linear regression we chose to eliminate these early warming periods as melt onset dates and used the 2nd (or 3rd, for O-Buoys 6 and 10, 2014) date reported through the melt onset algorithm, refer to Table 2.2 for all MODs. All dates were further verified through an additional algorithm analysis where a date was reported if $T_{\max} \geq 0^\circ\text{C}$ for a minimum of 5 days. This algorithm verified 11 out of the 12 dates, O-Buoy 10-2014 was the only site/year that did not have a date reported which after closer look found that the temperature dropped back below 0°C on the 5th day. After verification of MOD dates, a linear regression of the MOD and SED was performed.

To investigate the relationship between MOD and SED, a linear regression analysis was performed. Barrow 2009 and OB1 (2009) sites were located within 5 km of each other and had the same MOD and SED dates. Therefore, only Barrow 2009 was used for the linear regression analysis to prevent double counting. Figure 2.3 reveals a strong correlation between the MOD and SED for all sites, coastal (circle) and sea ice (triangle, $N = 11$, $R^2 = 0.989$, $slope = 0.925$, $intercept = 10$ days). Root mean square (RMS) of the difference between the MOD and SED (MOD – SED)

for all sites/years was 1.8 days. Figure 2.4 exhibits a histogram of the MOD-SED and yields a Gaussian relationship centered around zero. The average “bias” of the difference between MOD and SED was -0.3 days with a standard deviation of 1.77 days and standard error of 0.56 days.

2.3.3 Snow Depth Changes at Seasonal End and Recurrence Events

In four sea ice case studies, O-Buoy MAX-DOAS measurements were co-located with Ice-Mass Balance Buoys (Perovich et al., 2013), which allowed for an ancillary study of snow depth in relation to SED. As seen in Figure 2.5, all cases studies ($N=4$) show snow depth is nearly constant prior to the SED (black line); however, the snowpack height begins to decrease within 1-2 days of the SED. This decrease in snowpack height continues until about one day prior to the start of the recurrence event (left blue line, panels a, b, and c) and no change in depth is observed throughout the recurrence event. Snowpack decay is re-initiated after the end of the recurrence event (right blue line). The BrO relationship with decreasing snow depth appears to follow the air temperature behavior where the air temperature reaches 0°C within 1-2 days of the SED and the temperature decreases to below 0°C during the recurrence event, as reported above.

2.3.4 Rain/Snow Precipitation at Seasonal End and Recurrence Events

Routine weather observations (METAR) at Barrow, AK allow consideration of the weather relationship to the SED. Five total years were recorded, but 2008 data had measurement issues at the SED; therefore, only four years of data was used in the subsequent analysis. The first reported rain or freezing rain precipitation of each year at Barrow, AK occurred within one day of the SED in all cases ($N=4$). Figure 2.6 shows a four panel plot of Barrow years 2009 (panel a), 2012 (panel b), 2013 (panel c) and 2014 (panel d). The blue line is the SED, rain or freezing rain precipitation

event is the dashed green line (each dashed green line is a separate rain event), recurrence events are outlined in red lines and finally snow precipitation events after the seasonal end date are shaded in grey. Barrow in 2009 and 2012 had rain occur the same day as the SED; therefore, only one line is shown.

Recurrence events occurred in years 2012 and 2014. Figure 2.6 panel (b) shows Barrow in 2012 had two snow precipitation instances (shaded grey regions) before the recurrence event, on May 15-16th and again on May 20-21st; however, it rained (green dashed line) on May 17th, after the first snow precipitation event. The third snow precipitation event for Barrow in 2012 began one day prior to the recurrence start date (RSD) on May 24th and snowed throughout the recurrence event; followed by rain one day after the recurrence end date (RED) on May 30th. Barrow in 2014, panel (d) of Figure 2.6, had similar behavior; however, there was a longer multi-day snow precipitation event that occurred prior to the recurrence event from May 5th – May 9th, with subsequent rain on May 10th. Snow precipitation began one day prior to the RSD on May 17th and continued to snow throughout the recurrence event, followed by rain on June 1st, one day after the RED.

2.4 Discussion

2.4.1 Seasonal End Date is the Melt Onset Date

Near surface BrO is observed at warmer temperatures in this study than previously reported. We did not observe a temperature threshold of -15°C that was previously reported by Pöhler et al. (2010). They only observed BrO during its peak season in March – April of 2009 and did not experience temperatures warmer than -15°C during the 2009 field campaign. However, our temperature threshold of 0°C agrees with a recent study by Peterson et al. (2014), who observed

elevated BrO lower-tropospheric vertical column density (LT-VCD) up to -5°C . Additionally, ozone depletion events were observed at air temperatures up to -6°C by Bottenheim et al. (2009), circumstantially indicating BrO recycling was continually maintaining elevated BrO levels at warmer temperatures. Our results show that BrO recycling can occur up to 0°C ; however, as temperatures cross over 0°C BrO recycling ceases, possibly due to melt onset of the snowpack.

The correlation of MOD and SED dates, as seen in Figure 2.3, shows a strong correlation between these two dates, revealing that melt onset of the snowpack occurs within 2 days of the SED. Figure 2.4 shows the average difference between the MOD and SED was ~ 0 days and has little bias to which date occurs first. There were three sea ice sites (O-Buoys 4, 6, and 10-2015) that fell in the -3-day bin, which reveals the temperature date occurred three days prior to the SED. This suggests it may take longer for the sea ice snowpack to begin metamorphosing due to more stable temperatures, as compared to coastal snowpack that is more exposed to larger temperature fluctuations due to warmer airmasses from inland. Snowpack depth measured along with O-Buoy 10 (2015) showed a small dip in the snow depth one day before the SED which could support the theory that it takes longer for sea ice snowpack to begin metamorphosing; however, the relationship between temperature and snow depth needs a more thorough investigation. The strong correlation of the SED and MODs, with little variation and bias, suggests that melt onset inhibits BrO recycling, ending the reactive bromine season.

Rapid BrO recycling is dependent upon bromide ions at a solid surface, such as snow. Upon initiation of melt onset of a snowpack, bromide ions residing on snow grains would be the first to melt due to colligative properties and the ion pulse phenomenon. Liquid formation will begin to form at the location of any ions; therefore, ions would be the first to elute downward toward the base of the snowpack at the onset of melt (Bales et al., 1989; Johannessen and Henriksen, 1978).

Based on the theory that BrO recycling only occurs within the top 1 cm of the snowpack (Pratt et al., 2013), the onset of melt would remove majority of the bromide ions in the top 1 cm of the snowpack, needed to maintain BrO recycling, and re-distribute the ions towards the bottom of the snowpack which would limit bromide's availability for BrO recycling. However, it is unclear whether the ion pulse would completely inhibit BrO recycling because at least 20% of ions would remain in the top layer, based on the ion pulse phenomenon, and be able to participate in BrO recycling.

2.4.2 Decaying Snowpack and Rain Precipitation Prevents BrO Recycling

Based on the four case studies presented in Figure 2.5, we speculate that the decay of snow depth began 1 – 2 days after the SED is due to the increase in temperature and melt onset of the snowpack. Melting of the snowpack increases the liquid water content present on snow grains and subsequently coalesces snow grains (Brun, 1989; Colbeck, 1982) causing the snowpack height to decrease and the entire snowpack to become more compact. The compaction of snowpack is a large loss of surface area decreasing the total surface area of a snowpack by an order of magnitude (Dominé et al., 2002). In addition, the top of the snowpack will form a melt-freeze crust that has very little surface area (Dominé et al., 2007) and will decrease the ventilation of the snowpack (Albert and Perron, 2000). Although snow depth data at the coastal sites was not available, rain precipitation would induce snowpack decay due to the increase of liquid water content.

Rain or freezing rain precipitation occurred at almost every “end date” (SED and RED, $N = 6$), marking the onset of the melt season for those years at Barrow. Kwok et al. (2003) also reported that they had rain precipitation occur at a couple of their study sites in 1998 which marked the beginning of the melt season. Rain precipitation would increase liquid water content and

rapidly coalesce snow grains (Brun, 1989); therefore, surface area is quickly lost. Although we do not have snowpack depth data to confirm how much snow depth was lost during these rain precipitation events, we suggest that Barrow is losing snow depth at a similar, or slightly faster, rate as the O-Buoys.

2.4.3 Below Freezing Temperatures and New Surface Area Re-initialize BrO Recycling

Overall, recurrence events had more variability than the SED with respect to temperature. A variety of temperature metrics were explored to correlate with the recurrence event dates; however, no clear temperature metric was identified that could explain the temperature and recurrence event relationship. It is clear in the examples presented in Figure 2.1 that the temperature was below 0°C throughout the recurrence event and this was consistent for all five recurrence events observed (Barrow 2012 and 2014, O-Buoys 4, 10-2015, and 11). However, there were periods where the temperature was below 0°C but no recurrence event was observed. This suggests that temperature below freezing is necessary for BrO recycling; however, it is not sufficient to maintain BrO recycling. In addition to the necessary below freezing temperatures, ancillary snow depth measurements may be additionally aiding in BrO recycling.

Recurrence events occurred in three of the case studies (panels a, b, and d) presented in Figure 2.4. It appears in all three cases the snowpack depth remains nearly constant, no loss of depth or new accumulation, during the recurrence event (outlined in blue lines) The pause of snowpack decay is most likely due to the air temperature decreasing back below freezing, in which would form a melt-freeze crust. Re-frozen and metamorphosed snowpack would have significantly lower surface area than fresh fallen snow (Dominé et al., 2007). Similarly, a melt-freeze crust on top of the re-frozen snowpack would have drastically decreased ventilation throughout the

snowpack (Albert and Perron, 2000) and would reduce wind pumping that would allow for Br₂ to be released from the interstitial space of the snowpack (Morin et al., 2008; Pratt et al., 2013). Both the loss of surface and ventilation would not facilitate BrO recycling; however, recurrence events are observed during this period and it is possible there was new vapor-deposited surface area growth. The growth of surface hoar could have occurred due to the drop in temperature and deposition of vapor onto the surface of the melt-freeze crust (Gallet et al., 2014) which would have been small enough to not be detected by the sounder. The growth of surface hoar would increase the surface area of the melt-freeze crust available for BrO recycling by an order of magnitude (Dominé et al., 2007) which would facilitate BrO recycling; however, it is unclear as to whether there would be sufficient bromide available to maintain the recycling. We additionally speculate that recurrence events could be due to Br₂ release from sea salt aerosols or blowing snow that were transported to the measurement site (Mozurkewich, 1995; Frieß et al., 2011); however, aerosols and wind speed/direction were not analyzed in this study. Although it is unclear how snow depth may facilitate BrO recycling, ancillary snow precipitation data at coastal sites reveal snow may be necessary for re-initiation of BrO recycling.

Snow precipitation events occurred in both case studies with recurrence events. Barrow had a recurrence event in both 2012 and 2014, in which snow precipitation occurred throughout these recurrence events. However, there were shorter snow precipitation events that occurred prior to the recurrence event where BrO recycling did not re-initiate. This suggests that snow precipitation is necessary to re-initiate BrO recycling; however, it is not sufficient by itself. With only two cases where snow precipitation was observed during recurrence event, one should be cautious as to completely conclude new snow precipitation as a necessary component. Additional

analysis of snowfall and recurrence event with future measurements would give a better indication of this relationship.

2.5 Conclusion

Melt onset, snowpack depth and rain/snow precipitation were investigated in this study to understand their effects on BrO recycling. We were able to objectively determine the seasonal end date (SED) to the elevated reactive bromine season, as well as the temperature-based melt onset dates for all coastal and sea ice sites ($N=12$) from 2009 – 2015. The strong correlation of the MOD occurring within two days of the SED indicates that melt onset of the snowpack is hindering BrO recycling and ending the reactive bromine season. Ancillary snowpack depth analysis at sea ice sites revealed that the snowpack decay began approximately 1-2 days after the SED which supports that melt onset of the snowpack is inhibiting BrO recycling. Ancillary rain precipitation at coastal sites similarly agreed with snow depth data where rain precipitation occurred within one day of the SED and suggests that again there is a loss of snowpack surface area due to liquid water which is hindering BrO recycling.

Recurrence events, where BrO recycling is re-initialized, were much more variable than the SED. Snow depth analysis revealed no snow decay or accumulation occurred during the recurrence event; however, we speculate there may have been surface hoar growth or possible aerosol transport that could account for the BrO recycling. Snow precipitation at coastal sites revealed snow may be necessary to re-initialize BrO recycling but it is not sufficient alone.

If the start of the melt onset season is the end to the BrO season, this gives us an indication on how BrO may respond to future climate changes. Long term studies on the summer melt season found that the melt season has lengthened ~8 days per decade for Barrow, AK (Stone, 2002) and

~5 days for the pan-Arctic region (Markus et al., 2009). These summer melt trends and our results indicate that as the melt season lengthens, the BrO season will get shorter which would reduce the amount of ozone depletion events and mercury deposition during Arctic springtime.

2.6 Acknowledgements

The authors would like to thank Rick Thoman at NOAA, as well as Bruce Elder and Donald Perovich at CRREL for collaboration and providing measurement data. This research was supported by the Department of Chemistry and Biochemistry at University of Alaska Fairbanks, the National Aeronautics and Space Administration (NASA) Cryospheric Sciences Programs (CSP) and the National Science Foundation (NSF) under grant ARC-1023118.

2.7 References

- Abbatt, J. P. D., Thomas, J. L., Abrahamsson, K., Boxe, C., Granfors, A., Jones, A. E., King, M. D., Saiz-Lopez, A., Shepson, P. B., Sodeau, J., Toohey, D. W., Toubin, C., von Glasow, R., Wren, S. N. and Yang, X.: Halogen activation via interactions with environmental ice and snow in the polar lower troposphere and other regions, *Atmos. Chem. Phys.*, 12(14), 6237–6271, doi:10.5194/acp-12-6237-2012, 2012.
- Albert, M. R. and Perron, F. R.: Ice layer and surface crust permeability in a seasonal snow pack, *Hydrol. Process.*, 14(September), 3207–3214, 2000.
- Albert, M. R. and Shultz, E. F.: Snow and firn properties and air – snow transport processes at Summit Greenland, *Atmos. Environ.*, 36, 2789–2797, 2002.
- Anderson, M. R.: The Onset of Spring Melt in First-Year Ice Regions of the Arctic as Determined From Scanning Multichannel Microwave Radiometer Data for 1979 and 1980, *J. Geophys. Res.*, 92(13), 153 – 163, 1987.
- Bales, R. C., Davis, R. E. and Stanley, D. A.: Ion elution through shallow homogeneous snow, *Water Resour. Res.*, 25(8), 1869–1877, doi:10.1029/WR025i008p01869, 1989.
- Berg, W. W., Sperry, P. D., Rahn, K. A. and Gladney, E. S.: Atmospheric Bromine in the Arctic, *J. Geophys. Res.*, 88(3), 6719–6736, doi:10.1029/JC088iC11p06719, 1983.
- Bottenheim, J. W., Barrie, L. A., Atlas, E., Heidt, L. E., Niki, H., Rasmussen, R. A. and Shepson, P. B.: Depletion of lower tropospheric ozone during Arctic spring: The Polar Sunrise Experiment 1988, *J. Geophys. Res.*, 95(D11), 18555, doi:10.1029/JD095iD11p18555, 1990.
- Bottenheim, J. W., Netcheva, S., Morin, S. and Nghiem, S. V.: Ozone in the Boundary Layer air over the Arctic Ocean – measurements during the TARA expedition, *Atmos. Chem. Phys. Discuss.*, 9(2), 8561–8586, doi:10.5194/acpd-9-8561-2009, 2009.
- Brun, E.: Investigation on wet-snow metamorphism in respect of liquid-water content, *Ann. Glaciol.*, 13, 22–26, 1989.
- Carlson, D., Donohue, D., Platt, U. and Simpson, W. R.: A low power automated MAX-DOAS instrument for the Arctic and other remote unmanned locations, *Atmos. Meas. Tech.*, 3(5), 2347–2375, 2010.
- Colbeck, S. C.: An overview of seasonal snow metamorphism, *Rev. Geophys.*, 20(1), 45–61, doi:10.1029/RG020i001p00045, 1982.

- Dominé, F., Taillandier, A. S. and Simpson, W. R.: A parameterization of the specific surface area of seasonal snow for field use and for models of snowpack evolution, *J. Geophys. Res. Earth Surf.*, 112(2), 1–13, doi:10.1029/2006JF000512, 2007.
- Dominé, F., Cabanes, A. and Legagneux, L.: Structure, microphysics, and surface area of the Arctic snowpack near Alert during the ALERT 2000 campaign, *Atmos. Environ.*, 36(15-16), 2753–2765, doi:10.1016/S1352-2310(02)00108-5, 2002.
- Fan, S. M. and Jacob, D. J.: Surface ozone depletion in Arctic spring sustained by bromine reactions on aerosols, *Lett. to Nat.*, 359, 522–524, 1992.
- Frieß, U., Sihler, H., Sander, R., Phler, D., Yilmaz, S. and Platt, U.: The vertical distribution of BrO and aerosols in the Arctic: Measurements by active and passive differential optical absorption spectroscopy, *J. Geophys. Res. Atmos.*, 116(18), 1–19, doi:10.1029/2011JD015938, 2011.
- Gallet, J. C., Dominé, F., Savarino, J., Dumont, M. and Brun, E.: The growth of sublimation crystals and surface hoar on the Antarctic plateau, *Cryosphere*, 8(4), 1205–1215, doi:10.5194/tc-8-1205-2014, 2014.
- Hausmann, M. and Platt, U.: Spectroscopic measurement of bromine oxide and ozone in the high Arctic during Polar Sunrise Experiment 1992, *J. Geophys. Res.*, 99(D12), 25399, doi:10.1029/94JD01314, 1994.
- Holmes, C. D., Jacob, D. J. and Yang, X.: Global lifetime of elemental mercury against oxidation by atomic bromine in the free troposphere, *Geophys. Res. Lett.*, 33(20), 1–5, doi:10.1029/2006GL027176, 2006.
- Hönninger, G., von Friedeburg, C. and Platt, U.: Multi axis differential optical absorption spectroscopy (MAX-DOAS), *Atmos. Chem. Phys.*, 4, 231–254, 2004.
- Hönninger, G. and Platt, U.: Observations of BrO and its vertical distribution during surface ozone depletion at Alert, *Atmos. Environ.*, 36(15-16), 2481–2489, doi:10.1016/S1352-2310(02)00104-8, 2002.
- Huff, A. K. and Abbatt, J. P. D.: Kinetics and product yields in the heterogeneous reactions of HOBr with ice surfaces containing NaBr and NaCl, *J. Phys. Chem. A*, 106(21), 5279–5287, doi:10.1021/jp014296m, 2002.
- Johannessen, M. and Henriksen, A.: Chemistry of snow melt water: changes in concentration during melting, *Water Resour. Res.*, 14(4), 615–619, 1978.

- Knepp, T. N., Bottenheim, J., Carlsen, M., Carlson, D., Donohoue, D., Friederich, G., Matrai, P. M., Natcheva, S., Perovich, D. K., Santini, R., Shepson, P. B., Simpson, W., Stehle, R., Valentic, T., Williams, C. and Wyss, P. J.: Development of an autonomous sea ice tethered buoy for the study of ocean-atmosphere-sea ice-snow pack interactions: the O-buoy, *Atmos. Meas. Tech.*, 2(3), 249–261, doi:10.5194/amtd-2-2087-2009, 2010.
- Kwok, R., Cunningham, G. F. and Nghiem, S. V: A study of the onset of melt over the Arctic Ocean in RADARSAT synthetic aperture radar data, *J. Geophys. Res. Ocean.*, 108(C11), 3363, doi:10.1029/2002JC001363, 2003.
- Leser, H., Hönninger, G. and Platt, U.: MAX-DOAS measurements of BrO and NO₂ in the Marine Boundary Layer, *Geophys. Res. Lett.*, 30(10), 3–6, doi:10.1029/2002GL015811, 2003.
- Markus, T., Stroeve, J. C. and Miller, J.: Recent changes in Arctic sea ice melt onset, freezeup, and melt season length, *J. Geophys. Res. Ocean.*, 114(12), 1–14, doi:10.1029/2009JC005436, 2009.
- McConnell, J. C., Henderson, G. S., Barrie, L. A., Bottenheim, J. W., Niki, H., Langford, C. H. and Templeton, E. M. J.: Photochemical bromine production implicated in Arctic boundary-layer ozone depletion, *Nature*, 355, 150–152, doi:10.1038/355150a0, 1992.
- Morin, S., Marion, G. M., von Glasow, R., Voisin, D., Bouchez, J. and Savarino, J.: Precipitation of salts in freezing seawater and ozone depletion events: a status report, *Atmos. Chem. Phys.*, 8(3), 7317–7324, doi:10.5194/acpd-8-9035-2008, 2008.
- Mozurkewich, M.: Mechanisms for the release of halogens from sea-salt particles by free radical reactions, *J. Geophys. Res.*, 101(D 4), 9121–9138, 1995.
- Oltmans, S. J., Schnell, R. C., Sheridan, P. J., Perterson, R. E., Li, S. M., Winchester, J. W., Tans, P. P., Sturges, W. T., Kahl, J. D. and Barrie, L. A.: Seasonal surface ozone and filterable bromine relationship in the high Arctic, *Atmos. Environ.*, 23(11), 2431–2441, doi:10.1016/0004-6981(89)90254-0, 1989.
- Perovich, D., Richter-Menge, J. A., Elder, B., Arbetter, T., Claffey, K. and Polashenski, C.: Observing and understanding climate change: Monitoring the mass balance, motion, and thickness of Arctic sea ice, [online] Available from: <http://imb.erd.cdr.mil>, 2013.
- Peterson, P. K., Simpson, W. R., Pratt, K. A., Shepson, P. B., Frieß, U., Zielcke, J., Platt, U., Walsh, S. J. and Nghiem, S. V: Meteorological controls on the vertical distribution of bromine monoxide in the lower troposphere, *Atmos. Chem. Phys. Discuss.*, 14(17), 23949–23994, doi:10.5194/acpd-14-23949-2014, 2014.

- Platt, U. and Hönninger, G.: The role of halogen species in the troposphere., *Chemosphere*, 52(2), 325–38, doi:10.1016/S0045-6535(03)00216-9, 2003.
- Platt, U. and Janssen, C.: Observation and role of the free radicals NO₃, ClO, BrO and IO in the troposphere, *Faraday Discuss.*, 100, 175, doi:10.1039/fd9950000175, 1995.
- Pöhler, D., Vogel, L., Friess, U. and Platt, U.: Observation of halogen species in the Amundsen Gulf, Arctic, by active long-path differential optical absorption spectroscopy., *Proc. Natl. Acad. Sci. U. S. A.*, 107(15), 6582–6587, doi:10.1073/pnas.0912231107, 2010.
- Pratt, K. A., Custard, K. D., Shepson, P. B., Douglas, T. A., Pöhler, D., General, S., Zielcke, J., Simpson, W. R., Platt, U., Tanner, D. J., Gregory Huey, L., Carlsen, M. and Stirm, B. H.: Photochemical production of molecular bromine in Arctic surface snowpacks, *Nat. Geosci.*, 6(5), 351–356, doi:10.1038/ngeo1779, 2013.
- Richter, A., Wittrock, F., Eisinger, M. and Burrows, J. P.: GOME Observations of Tropospheric BrO in Northern Hemispheric Spring and Summer 1997, *Geophys. Res. Lett.*, 25(14), 2683–2686, 1998.
- Van Roozendaal, M., Wagner, T., Richter, A., Pundt, I., Arlander, D. W., Burrows, J. P., Chipperfield, M., Fayt, C., Johnston, P. V., Lambert, J. C., Kreher, K., Pfeilsticker, K., Platt, U., Pommereau, J. P., Sinnhuber, B. M., Tørnkvist, K. K. and Wittrock, F.: Intercomparison of BrO measurements from ERS-2 GOME, ground-based and balloon platforms, *Adv. Sp. Res.*, 29(11), 1661–1666, doi:10.1016/S0273-1177(02)00098-4, 2002.
- Simpson, W. R., von Glasow, R., Riedel, K., Anderson, P., Ariya, P., Bottenheim, J., Burrows, J., Carpenter, L., Frieß, U., Goodsite, M. E., Heard, D., Hutterli, M., Jacobi, H.-W., Kaleschke, L., Neff, B., Plane, J., Platt, U., Richter, A., Roscoe, H., Sander, R., Shepson, P., Sodeau, J., Steffen, A., Wagner, T. and Wolff, E.: Halogens and their role in polar boundary-layer ozone depletion, *Atmos. Chem. Phys.*, 7(2), 4375–4418, doi:10.5194/acpd-7-4285-2007, 2007.
- Simpson, W. R., Brown, S. S., Saiz-Lopez, A., Thornton, J. A. and Glasow, R. Von: Tropospheric Halogen Chemistry: Sources, Cycling, and Impacts, *Chem. Rev.*, 150312153236002, doi:10.1021/cr5006638, 2015.
- Steffen, A., Douglas, T., Amyot, M., Ariya, P., Aspö, K., Berg, T., Bottenheim, J., Brooks, S., Cobbett, F., Dastoor, A., Dommergue, A., Ebinghaus, R., Ferrari, C., Gardfeldt, K., Goodsite, M. E., Lean, D., Poulain, A. J., Scherz, C., Skov, H., Sommar, J. and Temme, C.: A synthesis of atmospheric mercury depletion event chemistry in the atmosphere and snow, *Atmos. Chem. Phys.*, 8(6), 1445–1482, doi:10.5194/acp-8-1445-2008, 2008.

Stone, R. S.: Earlier spring snowmelt in northern Alaska as an indicator of climate change, *J. Geophys. Res.*, 107(D10), doi:10.1029/2000JD000286, 2002.

Wagner, T., Leue, C., Wenig, M., Pfeilsticker, K. and Platt, U.: Spatial and temporal distribution of enhanced boundary layer BrO concentrations measured by the GOME instrument aboard ERS-2, *J. Geophys. Res.*, 106(D20), 24225, doi:10.1029/2000JD000201, 2001.

Winebrenner, D. P., Nelson, E. D., Colony, R. and West, R. D.: Observation of melt onset on multiyear Arctic sea ice using the ERS 1 synthetic aperture radar, *J. Geophys. Res.*, 99(C11), 22,425–22,441, doi:10.1029/94JC01268, 1994.

2.8 Figures

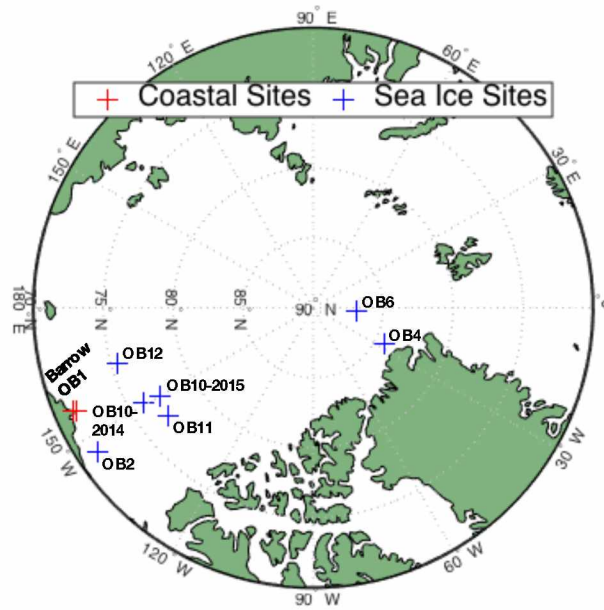


Figure 2.1: Pan-Arctic map of study site locations. The longitude and latitude of all sites can be found in Table 2.2.

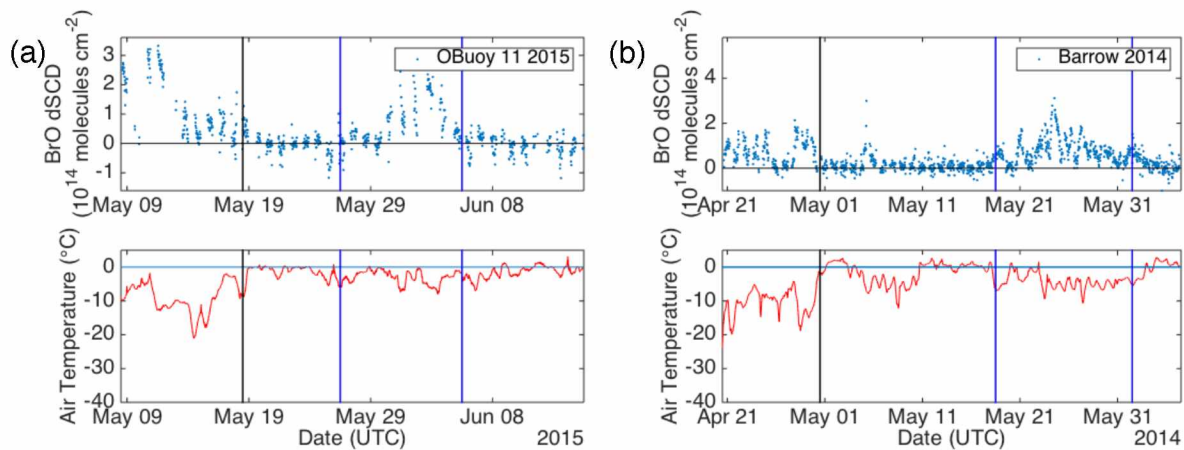


Figure 2.2: Sea Ice (panel a, O-Buoy 11-2015) and coastal (panel b, Barrow 2014) case study sites that represent the typical relationship between BrO (top subplot) and temperature (bottom subplot) during late spring (May – June). Seasonal end date (SED) is displayed as the black vertical line, and the recurrence event is outlined with two vertical blue lines.

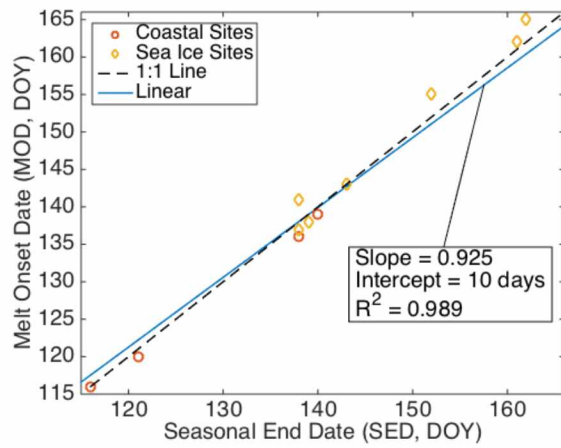


Figure 2.3: Linear regression analysis of the seasonal end date (SED) and melt onset date (MOD). Strong correlation is found between the SED and MOD for all sites ($N = 11$) with a R^2 of 0.989. O-Buoy 1 2009 was removed from this analysis to prevent double counting.

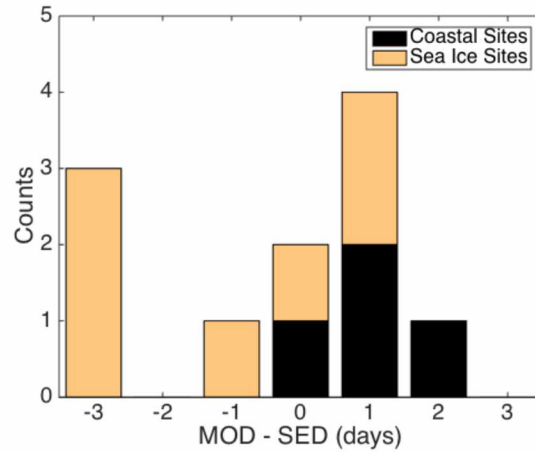


Figure 2.4: Histogram of the difference between the melt onset date (MO) and seasonal end date (SED). The calculated average of all MO-SED ($N = 11$) is -0.36 days with a standard deviation and error of 1.77 days and 0.56 days, respectively. O-Buoy 1 2009 was removed from this analysis to prevent double counting.

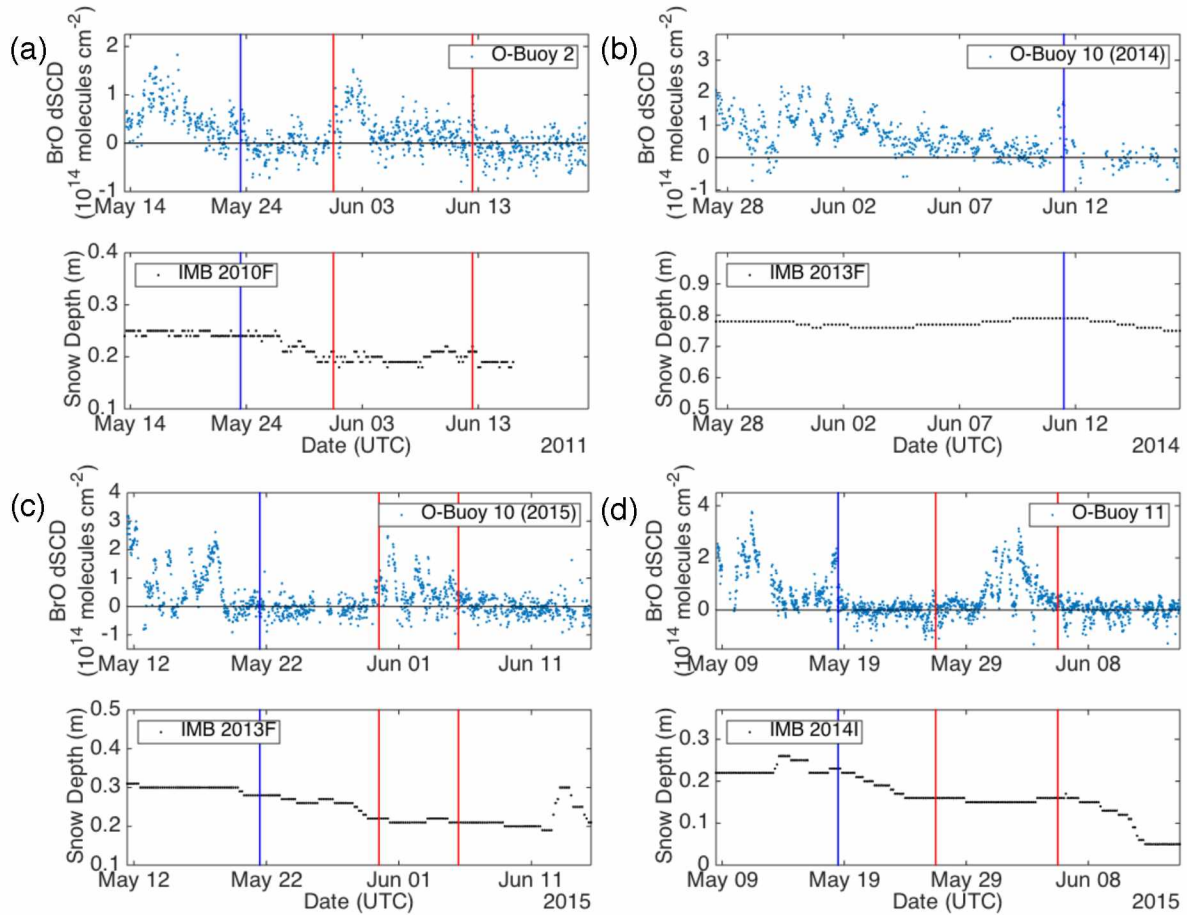


Figure 2.5: BrO 2° elevation angle dSCD (top subplot) and snow depth (bottom subplot) for three separate O-Buoys and co-located ice-mass balance buoys (IMBs) (panel a, b/c, and d). O-Buoy 10 and IMB 2013F collected two years of late spring data from 2014 (panel b) and 2015 (panel c). The SED (blue line) and recurrence events (outlined in red lines, panels (a), (c) and (d)) are pictured as the blue line and outlined in red lines, respectively.

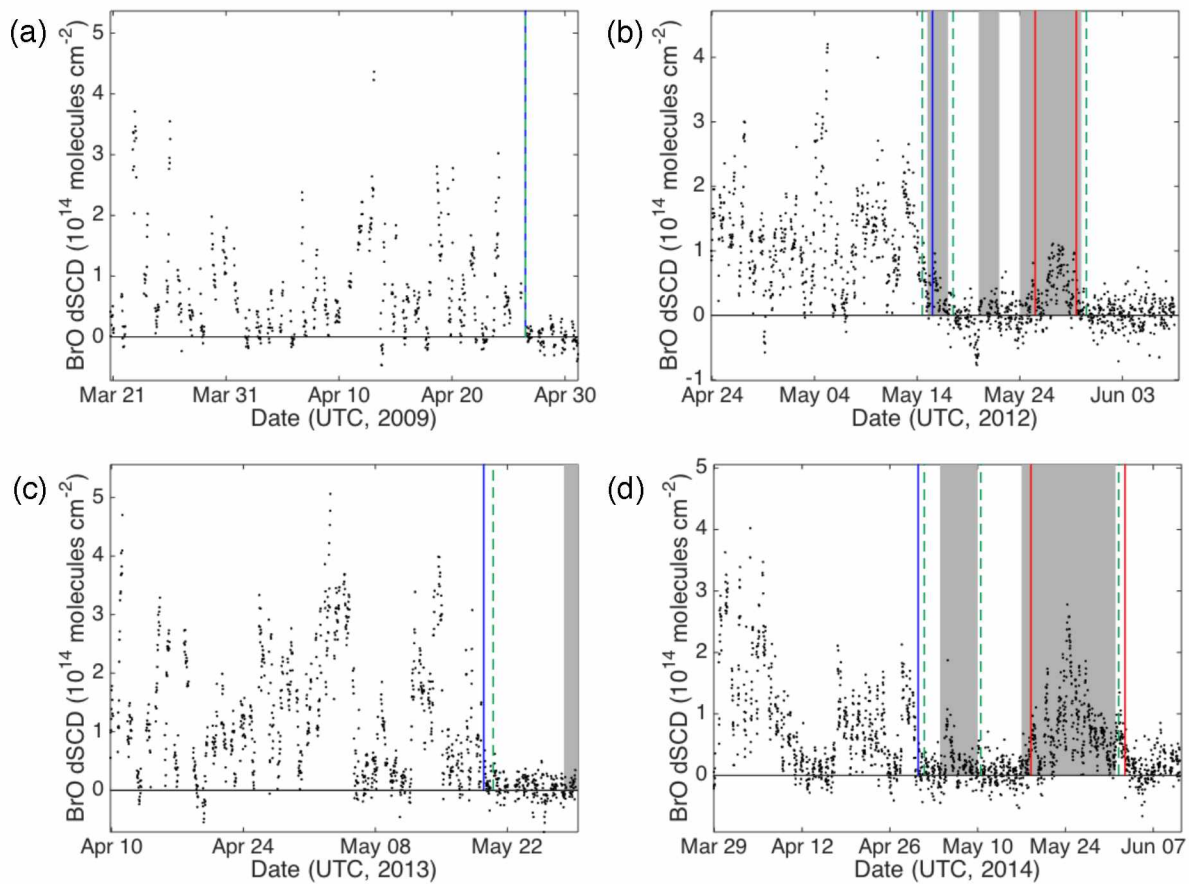


Figure 2.6: Rain and snow precipitation events at Barrow, AK for 2009 (panel a), 2012 (panel b), 2013 (panel c) and 2014 (panel d). SED (blue line) and recurrence events (outlined in red lines) are pictured, including rain (green dashed line) and snow precipitation events (grey shaded regions). The SED and rain precipitation event occurred on the same day for Barrow 2009 (panel a); therefore, only one line is present.

Table 2.1: Seasonal, recurrence and melt onset dates for all sites and years.

Category	Site (Year)	Co-located Buoy (Perovich et al., 2013)	Longitude (°W)	Latitude (°N)	Seasonal End Date (SED)	Melt Onset Date (MOD)	Recurrence Start Date (RSD)	Recurrence End Date (RED)
Coastal	Barrow (2009)		156.6809	71.3274	26-Apr-2009 (116)	26-Apr-2009 (116)		
	O-Buoy 1 (2009)		156.341	71.541	26-Apr-2009 (116)	26-Apr-2009 (116)		
	Barrow (2012)		156.6679	71.3249	15-May-2012 (136)	17-May-2012 (138)	25-May-2012 (146)	29-May-2012 (150)
	Barrow (2013)		156.6679	71.3249	19-May-2013 (139)	20-May-2013 (140)		
	Barrow (2014)		156.6679	71.3249	30-Apr-2014 (120)	1-May-2014 (121)	18-May-2014 (138)	02-Jun-2014 (153)
Sea Ice	O-Buoy 2 (2011)	2010F	146.2986	74.4716	23-May-2011 (143)	23-May-2011 (143)	02-May-2009 (122)	*
	O-Buoy 4 (2012)		26.4955	84.3632	03-Jun-2012 (155)	31-May-2012 (152)	31-May-2011 (151)	12-Jun-2011 (163)
	O-Buoy 6 (2012)		5.2927	86.8946	13-Jun-2012 (165)	10-Jun-2012 (162)		
	O-Buoy 10 (2014)	2013F	150.5937	76.1514	11-Jun-2014 (162)	10-Jun-2014 (161)		
	O-Buoy 10 (2015)	2013F	150.1518	77.4246	21-May-2015 (141)	18-May-2015 (138)	30-May-2015 (150)	05-Jun-2015 (156)
	O-Buoy 11 (2015)	2014F	143.1906	77.1001	18-May-2015 (138)	19-May-2015 (139)	26-May-2015 (146)	05-Jun-2015 (156)
	O-Buoy 12 (2015)		164.1501	75.4811	17-May-2015 (137)	18-May-2015 (138)		

*MAX-DOAS instrument stopped working before the RED was observed

Table 2.2: Noise threshold values and seasonal end date (SED) sensitivity test results for all sites and years.

Site (Year)	Noise Threshold (1×10^{13})	Consecutive Days (ST1)					BrO Threshold (1×10^{13} , ST2)						
		3	4	5	6	7	3.5	4	4.5	5	5.5	6	6.5
Barrow(2009)	2.50	116	116	116	*	*	116	116	116	116	116	116	116
Barrow(2012)	3.25	136	136	136	136	136	137	137	137	136	136	136	136
Barrow(2013)	2.50	139	139	139	139	139	143	140	140	139	139	139	139
Barrow(2014)	2.75	120	120	120	120	120	*	127	125	120	120	120	120
O-Buoy 1(2009)	1.75	116	116	116	116	*	116	116	116	116	116	116	116
O-Buoy 2(2011)	3.50	143	143	143	143	143	143	143	143	143	143	143	143
O-Buoy 4 (2012)	1.00	155	155	155	155	155	162	155	155	155	155	153	153
O-Buoy 6 (2012)	2.50	161	165	165	165	165	*	167	167	165	161	161	161
O-Buoy 10 (2014)	3.00	162	162	162	*	*	162	162	162	162	162	162	162
O-Buoy 10 (2015)	2.75	141	141	141	141	141	141	141	141	141	138	138	138
O-Buoy 11 (2015)	3.25	138	138	138	138	138	138	138	138	138	138	138	138
O-Buoy 12 (2015)	2.25	137	137	137	143	143	138	137	137	137	137	137	137

* No date was reported by the algorithm

3.1 Conclusions

Bromine Monoxide and ozone seasonality have shown BrO rapidly decrease as O₃ increases during late spring (May-June) in the Arctic. Late spring yields environmental changes that would hinder BrO recycling, including temperature increases, snowpack melting and rain precipitation. Recent studies have shown the importance of saline snow to BrO recycling; however, as temperature increases and snowpack melt onset begins ions at the top and middle of the snowpack are re-distributed down the snowpack due to ion pulse. In addition, as the temperature increases to freezing, snow grains start to coalesce, dramatically decreasing the surface area. After melting of the snowpack begins, melt-freeze crusts can form due to the temperature fluctuations. Melt-freeze crust has very little surface area, compared to fresh snow, and can effectively decrease the ventilation of the snowpack which both can inhibit BrO recycling.

The results presented in this thesis confirm that the start of the melt season, when temperature reaches 0°C, in the Arctic is the end of the reactive bromine season. There are a variety of changes that take place at the onset of melt, including snowpack decay and rain precipitation, in which both began within 1 – 2 days of the BrO seasonal end. Melt onset is a crucial time where snow surface area is decreasing and ions would be lost due to elution. We were not able to identify which factor was eliminated first, surface area or bromide ions; however, we speculate that both may be happening simultaneously. Although there were a few case studies where the temperature reached 0°C but no “irreversible physical changes” to the snowpack occurred, the seasonal end to reactive bromine and start of the melt season occurred within 1 – 2 days of each other. With an Arctic dominated by first-year ice and a longer summer season, its possible the BrO season will

get shorter and less ozone depletion events and mercury deposition will be observed during Arctic springtime.

3.2 Future Outlook

This study defined melt onset solely on air temperature data, which overall is not the ideal metric for determining melt onset; however, an ancillary satellite detection study of melt onset, similar to studies by Winebrenner et al. (1994) and Kwok et al. (2003), would help to confirm that melt onset is occurring at the same time as the reactive bromine seasonal end. In addition, spectral albedo changes, that indicate snow grain size, would be an additional analysis that could confirm melt onset of snowpack. Wind direction and speed were not analyzed in this study; however, understanding the wind behavior during the seasonal end date (SED) and recurrence events could be a great indication of what influence wind has on these events. Wind direction at the coastal sites could be useful to understand if the melt onset of the snowpack was due to the transport of warm temperature airmasses from inland. Large temperature fluctuations were seen at coastal sites, so it is possible this is due to the direction of wind.

Recurrence events were much more variable than the SED and could give us more information on how BrO recycling is being re-initiated. Wind direction and aerosol extinction would be a useful future study to see if recurrence events are due to aerosols. Aerosol research suggests that sea salt aerosols and snow/ice particles, that had contact with first year ice and/or potential frost flowers, are transported to the measurement site where Br₂ is subsequently released (Frieß et al., 2011). Although we did observe snow precipitation in both case studies at Barrow, it would be useful to understand fresh snowfall's role in BrO recycling. New snowfall is relatively "pure" of bromide; however, it is possible that it takes little time for new snowfall to build up

enough bromide to re-initiate BrO recycling. Although we uncovered some new and exciting results from this study, there is a lot more research to do and questions to ask about the environmental controls of BrO recycling.

3.3 References

- Frieß, U., Sihler, H., Sander, R., Pohler, D., Yilmaz, S. and Platt, U.: The vertical distribution of BrO and aerosols in the Arctic: Measurements by active and passive differential optical absorption spectroscopy, *J. Geophys. Res. Atmos.*, 116(18), 1–19, doi:10.1029/2011JD015938, 2011.
- Kwok, R., Cunningham, G. F. and Nghiem, S. V: A study of the onset of melt over the Arctic Ocean in RADARSAT synthetic aperture radar data, *J. Geophys. Res. Ocean.*, 108(C11), 3363, doi:10.1029/2002JC001363, 2003.
- Winebrenner, D. P., Nelson, E. D., Colony, R. and West, R. D.: Observation of melt onset on multiyear Arctic sea ice using the ERS 1 synthetic aperture radar, *J. Geophys. Res.*, 99(C11), 22,425–22,441, doi:199410.1029/94JC01268, 1994.